

UNIVERSITY OF COLORADO - BOULDER

ASEN 3802: AEROSPACE SCIENCES LABORATORY II

FEBRUARY 15TH, 2024

Lab 1: Structural Mechanics

Author:

JORDAN RICHARDSON

Author:

ZACHARY SELLECK

Author:

BRADY SIVEY

Author:

JARED STEFFEN

Professor:

ERIK KNUDSEN



Ann and H.J. Smead
Aerospace Engineering Sciences
UNIVERSITY OF COLORADO **BOULDER**

I. Introduction

The primary objective is to demonstrate how the integration of real-world measurements with computer simulations can provide insights into the behavior of structures under varying conditions. Specifically, the focus is on a 3D 16-bay truss subjected to static loading, akin to scenarios found in beam-like support setups.

The data collected from experiments will be compared with what is expected from theoretical models. The software ANSYS was used to run simulations based on the Finite Element Method. This software allows for the creation of detailed digital models of the truss and examination deflection, reaction forces, and internal forces in response to various loading scenarios.

The analytical model was hand derived and the truss was assumed to be an equivalent beam for this model. Utilizing the derived analytical model, our objective is to ascertain the loading conditions for two additional scenarios primarily relying on reaction forces. The initial scenario involves a load applied at a single node positioned away from the center. Subsequently, the second scenario presents the challenge of identifying two equal loads applied at unknown nodes within the truss structure.

By conducting these analyses, the aim is to not only assess the accuracy of the models but also to gauge the sensitivity of predictions to factors such as variations in material properties and experimental data. This approach allows for a thorough examination of the impact of potential sources of error, including imperfect joints, free-play in load cells, friction at joints, manufacturing imperfections, and assumptions regarding stress distribution.

II. Methodology

A. MoI Calculation

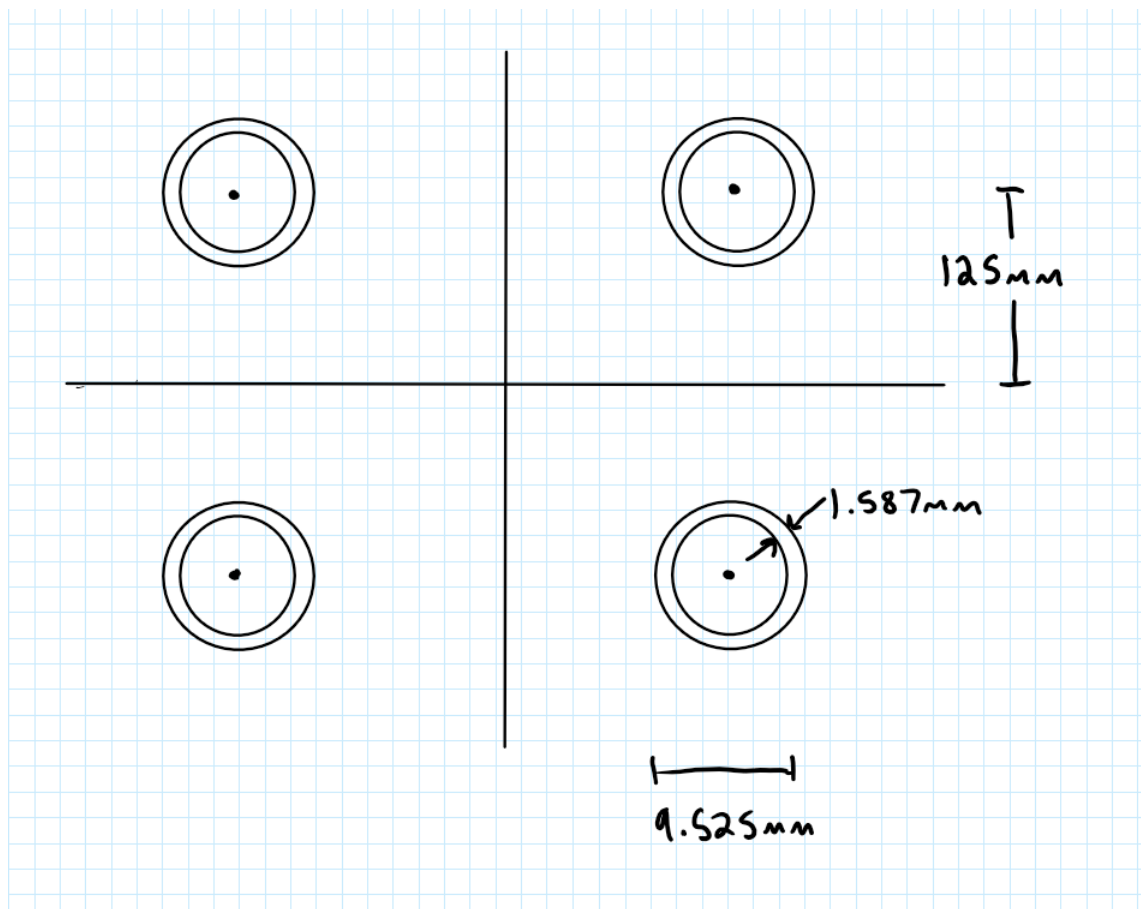


Fig. 1 Beam Equivalent Model Cross Section

For the analytical model, the truss was modeled as an equivalent beam, only considering the four struts that go the entire length of the truss and not the diagonal two force members. Figure 1 has the dimensions for the cross-sectional area of this equivalent beam model. Parallel-axis theorem was then used on the cross-section to find the area moment of inertia. The final result after using the parallel axis theorem was $2.476 \times 10^{-6} m^4$. Below are the equations used and tabulated results for determining the area moment of inertia.

1. Equations

$$A_{ring} = \pi(r_{outer}^2 - r_{inner}^2)$$

$$I_z = \frac{\pi}{2}(r_{outer}^4 - r_{inner}^4)$$

$$I_z = \Sigma \bar{I}_z + Ad^2$$

2. Mol Table

Table 1 Area Moment of Inertia Tabulated Data

Segment	Area (A) [m^2]	Distance (d) [m]	Ad^2 [m^4]	I_z [m^4]
1	3.957×10^{-5}	0.125	6.183×10^{-7}	6.483×10^{-10}
2	3.957×10^{-5}	0.125	6.183×10^{-7}	6.483×10^{-10}
3	3.957×10^{-5}	0.125	6.183×10^{-7}	6.483×10^{-10}
4	3.957×10^{-5}	0.125	6.183×10^{-7}	6.483×10^{-10}
Σ	—	—	2.473×10^{-6}	2.593×10^{-9}

B. Beam Bending Derivation

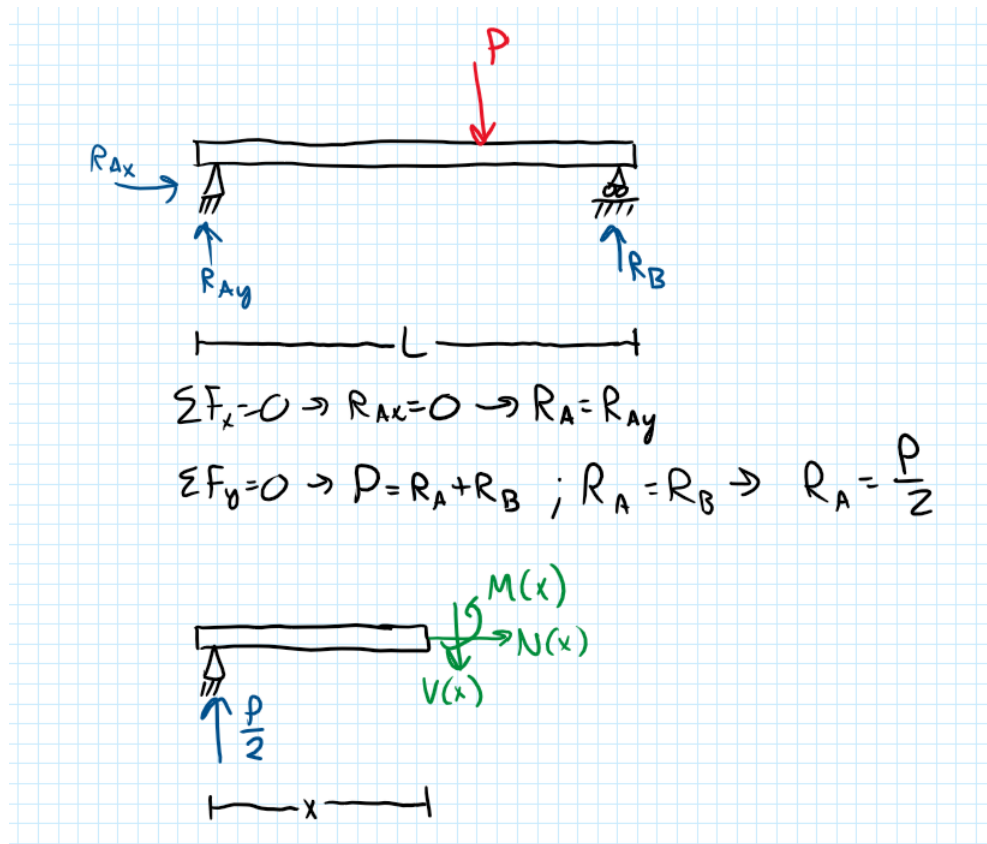


Fig. 2 Beam Bending FBD

The FBD in Figure 2 was used to perform a statics calculation to determine $M(x)$, which in turn can lead to $v(x)$, the beam deflection up to the midpoint of the truss.

$$\Sigma M_x = M(x) - \frac{P}{2}x = 0 \therefore M(x) = \frac{P}{2}x$$

$$\Theta(x) = \frac{1}{EI} \int M(x) dx = \frac{1}{EI} \left[\frac{P}{4}x^2 + C_1 \right]$$

$$v(x) = \frac{1}{EI} \int \Theta(x) dx = \frac{1}{EI} \left[\frac{P}{12}x^3 + C_1x + C_2 \right]$$

At the midpoint of the truss $\Theta = 0$ and at the beginning of the truss $v = 0$. Therefore:

$$\Theta(2) = \frac{1}{EI} [P + C_1] = 0 \therefore C_1 = -P$$

$$v(0) = \frac{1}{EI} C_2 = 0 \therefore C_2 = 0$$

$$\therefore v(x) = \frac{1}{EI} \left[\frac{P}{12}x^3 - Px \right]$$

III. Results

A. Question 1: Experimental results

1. Experimental Data Analysis

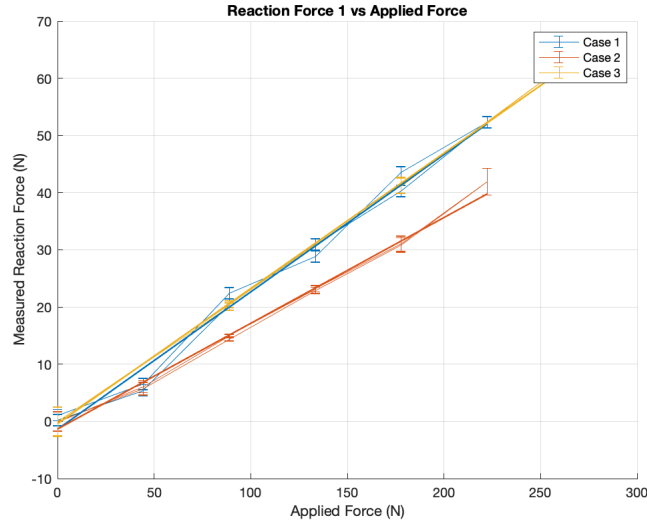


Fig. 3 Experimental Reaction Force 1 for All 3 Cases with Error Bars

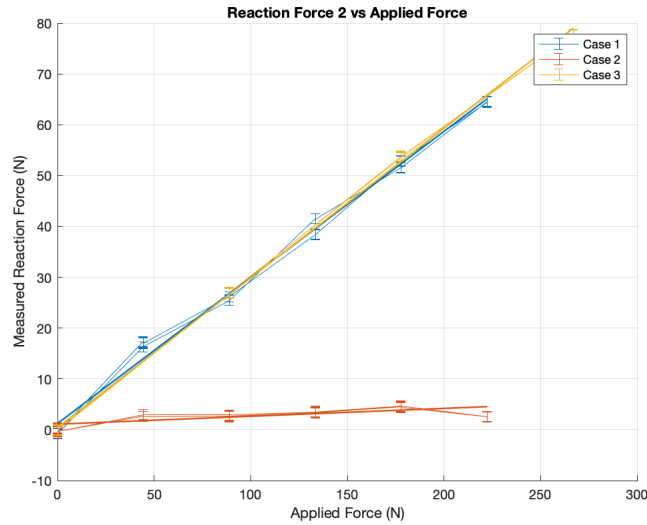


Fig. 4 Experimental Reaction Force 2 for All 3 Cases with Error Bars

Figures 3 and 4 show the reaction forces at one end of the truss as a function of increasing applied load. For cases 1 and 3, the loading curves have similar values and slopes for each sensor. This makes sense because the loads are determined to be at the midpoint of the truss for both of these cases. This is given to us for the first case, and the derivation for the third case can be seen in Appendix A. Regarding the second case, the most probable reason for why the reaction forces are different is due to the fact that the load is off center. This is explored more in depth in question 3.

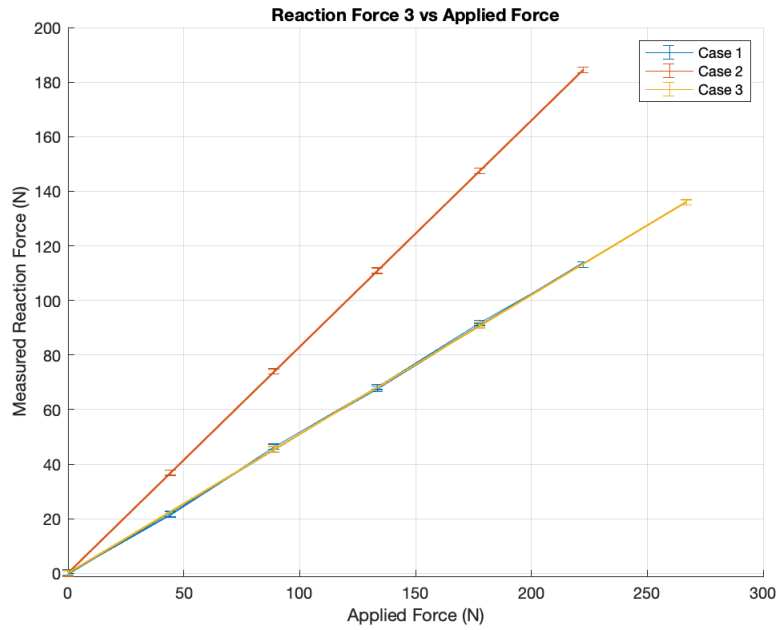


Fig. 5 Experimental Reaction Force 3 for All 3 Cases with Error Bars

Figure 5 shows the reaction force at the other end of the truss as a function of increasing applied load. Case 1 and 3 show a very similar loading trend while case 2 exhibits a much higher load as compared to the two. This means that for case 2, it can be inferred that the load was placed much closer to load sensor 3 as compared to load sensor 1 or 2. Further, it can be seen that based on these results and the results from figures 3 and 4, the loading distribution is very similar for cases 1 and 3 and can be predicted to be positioned near the center of the truss.

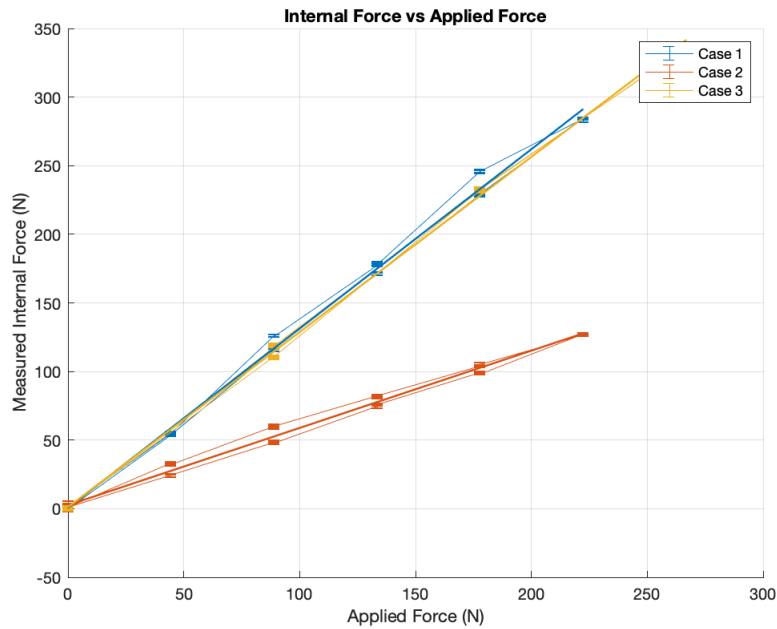


Fig. 6 Experimental Internal Forces for All 3 Cases with Error Bars

Figure 6 shows the internal force within the truss at the lengthwise midpoint as a function of increasing applied load. For cases 1 and 3, the internal force is very similar throughout. However, case 2 shows much lower internal forces. This makes sense because it's been assumed that the resultant force for case 2 is not centered at the middle while case 1 and 3 show a likelihood to have a resultant force positioned in the center. Because the internal force is measured at the midpoint, it makes sense that it would be less for case 2 as compared to cases 1 and 3.

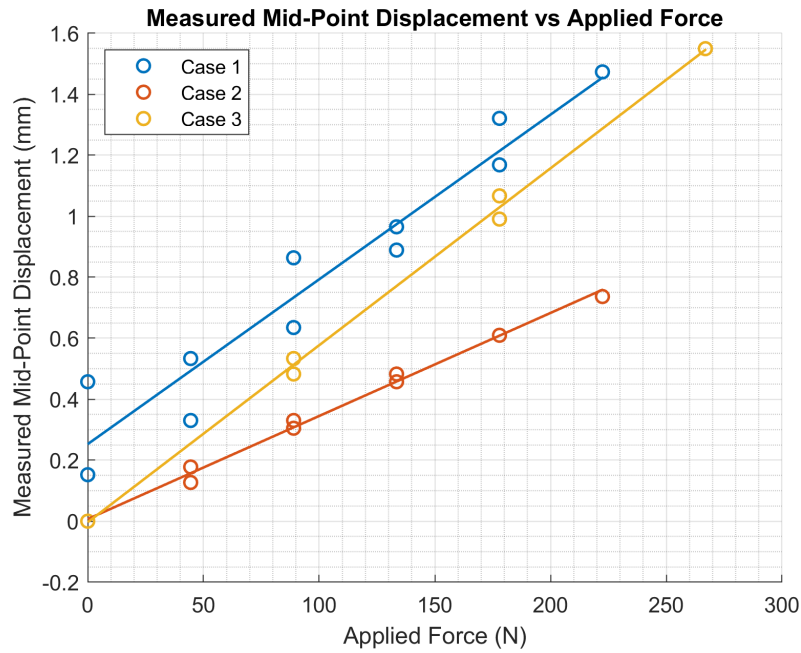


Fig. 7 Experimental Midpoint Displacement For All 3 Cases

Figure 7 shows the mid-point displacement as a function of increasing applied force. Right away it should be noted that case 1 shows an initial displacement at zero loading. This could be due to the sensor not being zeroed before measurements were taken. Conversely, case 2 and 3 both start at zero, however case 3 has much more overall displacement than case 2 and similar overall displacement to case 1. This makes sense because, again it was inferred that the resultant loading for cases 1 and 3 is centered at the midpoint which would give the greatest displacement where the sensor is located.

Table 2 Experimental Data

Measurement	Case 1	Case 2	Case 3
Reaction Force 1 [N]	52.3289	41.9289	63.5651
Reaction Force 2 [N]	64.5837	4.6528	77.7282
Reaction Force 3 [N]	113.2428	184.4411	135.9465
Internal Midpoint Force [N]	284.6328	127.4980	337.1094
Midpoint Displacement [mm]	1.4732	0.7366	1.5494

2. Linear Regression and Uncertainty Analysis

Table 3 R Squared Values

Model	Case 1	Case 2	Case 3
Reaction Force 1	0.9857	0.9940	0.9995
Reaction Force 2	0.9935	0.5637	0.9993
Reaction Force 3	0.9997	1.0000	1.0000
Internal Midpoint Force	0.9959	0.9908	0.9989
Midpoint Displacement	0.9272	0.9952	0.9978

The lines of best fit were determined through the least squares method for all of the plots is Figures 3-7. Tables 3 shows the R Squared values for the linear regression model fitted to the experimental data for all of the sensors. By looking at the table, almost all of the values are very close to 1 which represents a perfectly fitting linear regression line to the data. This thereby verifies the linearity of the measurements versus external load magnitude.

Figures 3-6 show error bars based on the standard deviation at each point. For all of the cases, the linear regression models are well within these error bars. This further proves the linearity of the regression line and the data.

B. Question 2: Comparison with analytical and FEM results

1. Analytical Results

Through the use of statics, the reaction forces at each corner of the truss were calculated to be $55.6N$. Additionally, the internal forces, which were assumed to be constant through the bars, were calculated to be equal to the load, which was $222.4N$. Using the values of $E = 70GPa$, $P = 222.4N$, and $I = 2.476 \times 10^{-6}m^4$, $x = 2m$ as well as the derived equation for $v(x)$, the magnitude of the deflection at the midpoint comes out to be $0.001711m$ or $1.71mm$

2. FEM Results

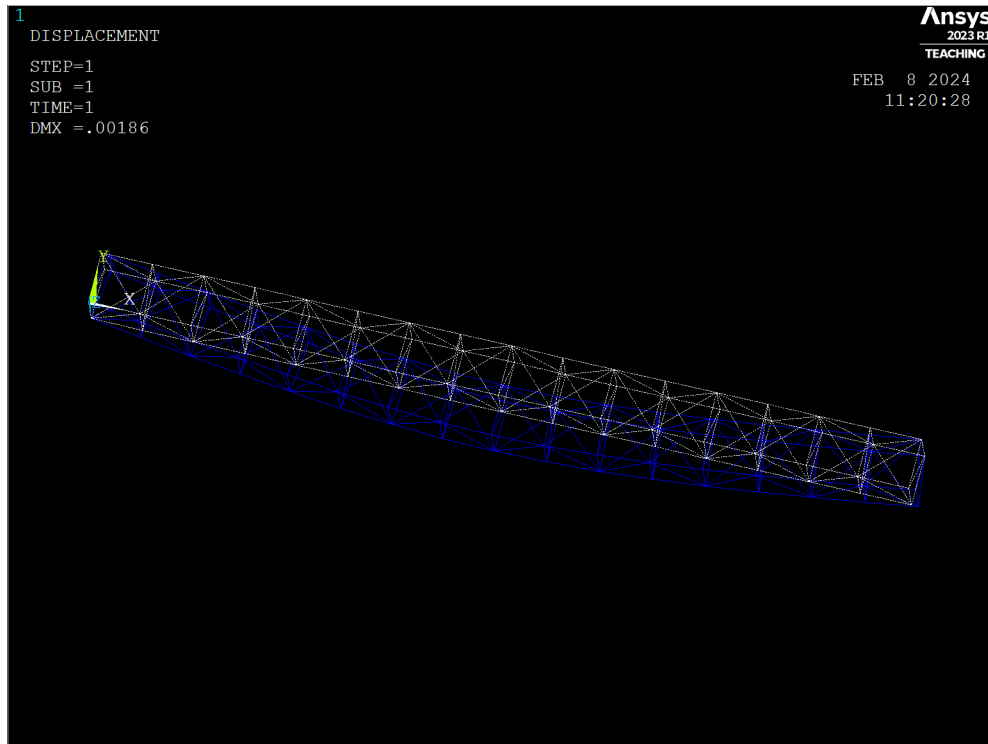


Fig. 8 Deformed vs Undeformed Truss Structure (Exaggerated)



Fig. 9 Internal Forces Contour Plot

Figures 8 and 9 show the deformed vs undeformed truss and the contour plot for the internal forces respectively. With a force of $-111.2N$ acting on each of the middle nodes, the truss had a midpoint deflection of $1.85mm$. The maximum internal force was found to be $450.14N$ with reaction forces right around $55.6N$ for each corner joint connected to a supporting joint.

3. Comparison

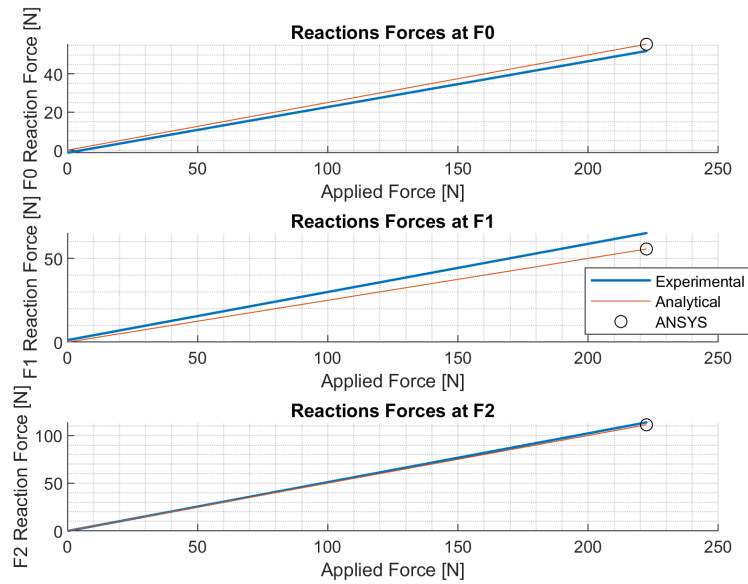


Fig. 10 Reaction Force Comparison For All 3 Models

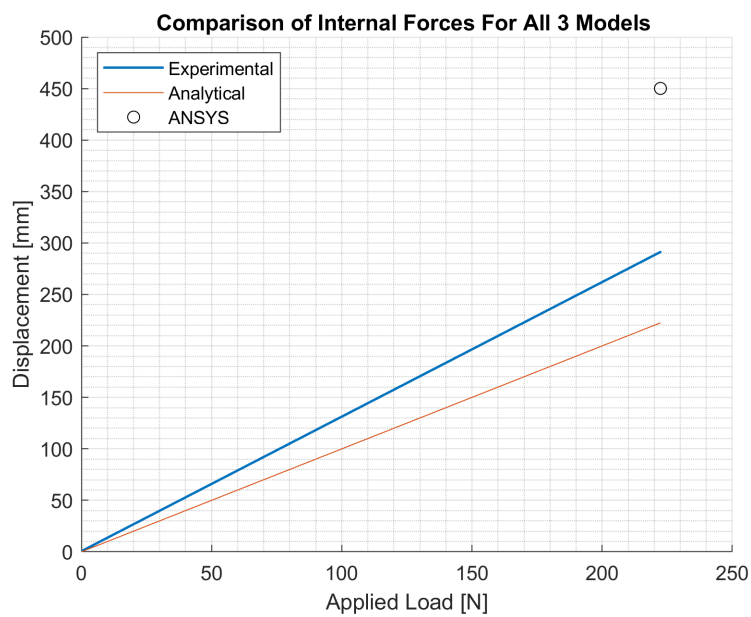


Fig. 11 Internal Force Comparison For All 3 Models

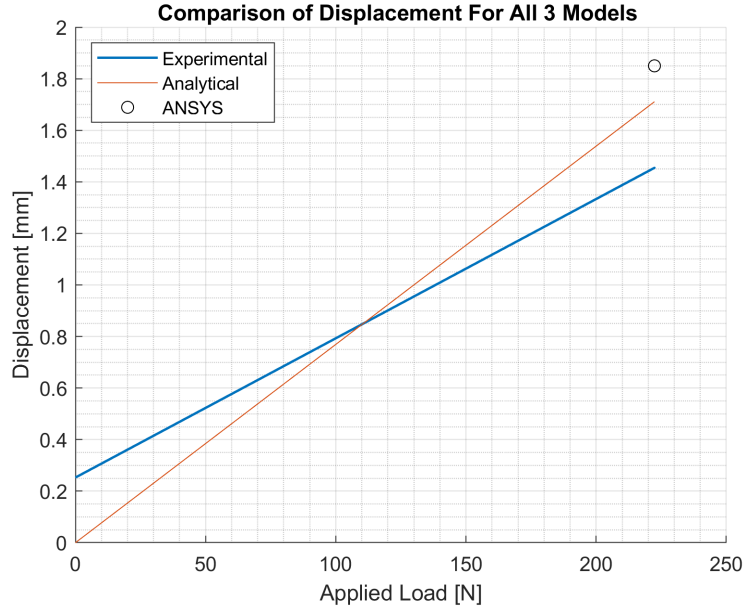


Fig. 12 Midpoint Displacement Comparison For All 3 Models

Figures 10-12 depict the graphical results of all 3 models. Note that the FEM model only tested the maximum loading scenario, which is why there is only one data point at the maximum loading of 222.4N. The two tables below show the numerical results as well as the percent errors for each model compared to the experimental data. For the analytical model, the midpoint displacement sees a 17.61% error, while the internal forces see a 23.65% error. The reaction forces are much smaller, with 6.86%, 14.63%, and 2.19% for F0, F1, and F2. For the ANSYS analysis, quite a large difference in midpoint deflection and maximum internal force, with 23.65% and 54.54% differences. The reaction forces have much smaller percent error, similar to the analytical model, with 6.78%, 14.59%, and 2.21% for F0, F1, and F2.

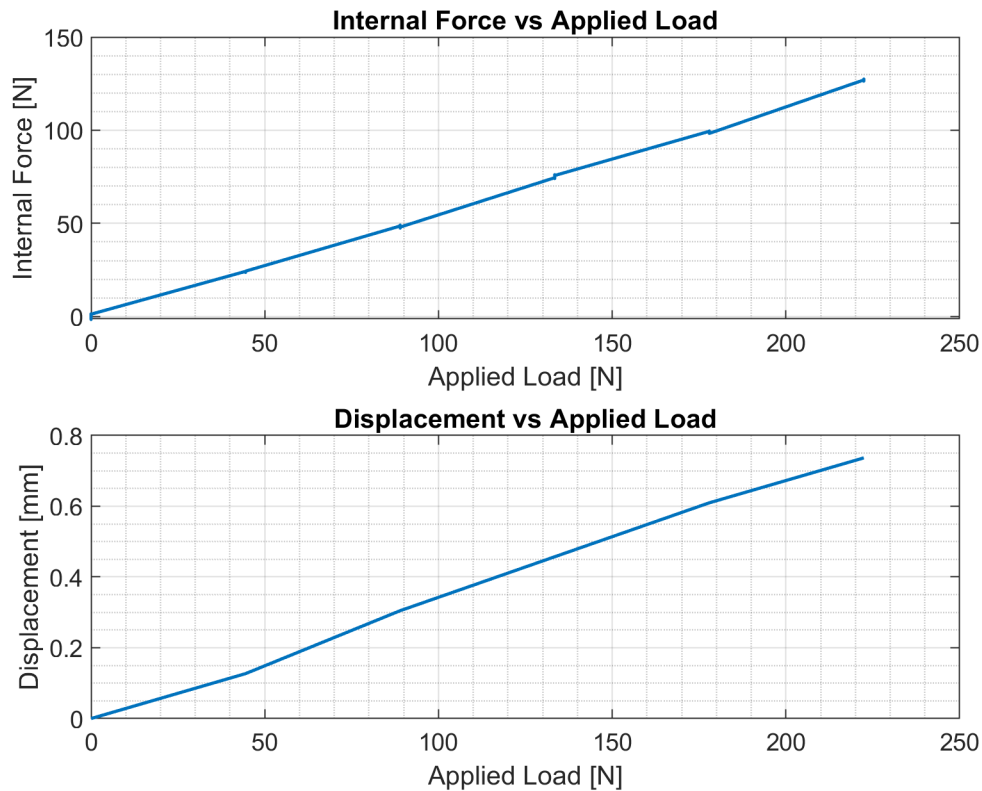
The main reasons behind the differences between the experimental results and the analytical and FEM models is due to sources of error, which are talk about in section IV, and due to the simplifications and assumptions made to make analysis of the models easier. The main assumptions for the analytical model include the fact that the truss is made of only 4 struts that run the full length of the structure, as well as no friction at the supports. The main assumptions for the FEM model are that the struts actually are links rather than beams, and that every joint in the truss is perfect and allows no free-play.

Table 4 Comparison from Experimental Data

Model	Midpoint Displacement [mm]	Max Internal Force [N]	Reaction Forces [N]
Experimental	1.45	291.31	F0: 52.03 F1: 65.13 F2: 113.79
Analytical	1.71	222.40	F0: 55.6 F1: 55.6 F2: 111.20
FEM	1.85	450.14	F0: 55.56 F1: 55.63 F2: 111.19

Table 5 Percent Error from Experimental Data

Model	Midpoint Displacement Error	Max Internal Force Error	Reaction Forces Error
Analytical	17.61%	23.65%	F0: 6.86% F1: 14.63% F2: 2.19%
FEM	27.24%	54.54%	F0: 6.78% F1: 14.59% F2: 2.21%

C. Question 3: Using modeling to identify the other loading conditions*1. Loading Case 2***Fig. 13 Internal Force and Displacement For Loading Case 2**

For the first unknown loading case, there was one load at a unknown location with the reaction forces, midpoint deflection, and internal forces given from the experimental data. It was possible to determine the loading location due to the fact that there was only one unknown, the loading location distance from the start of the truss. The derivation for determining this loading placement using statics can be seen in Appendix A, but the resulting equation for the location of the load was:

$$a = \frac{R_B L}{P}$$

The final resulting location was at $3.31m$. Knowing that the loads could only be placed at increments of $0.25m$, it is safe to assume that the actual loading position was at $3.25m$. Putting this value into the equivalent beam model,

the resulting deflection at the midpoint if the load is at $3.25m$ is $0.24mm$, while the actual result was $0.7366mm$. This yields a 66.38% error.

The experimental midpoint internal force was $127.5N$. For the equivalent beam model, the internal force is assumed to be constant through the whole bar, with a magnitude of $222.4N$. This yields a 74.43% error. These results indicate that the equivalent beam model is not an accurate model if the displacement is off center like it is in the second case. The assumed reason for such a large percent error between the experimental and equivalent beam model is due to the fact that the bending stiffness provided by the struts and the bending moments transmitted by the joints are going to be different to the left and right of the load when the load is off center and the equivalent beam model doesn't account for either of these. The experimental data for midpoint displacement and internal force at the middle of the truss can be seen in Figure 13.

2. Loading Case 3

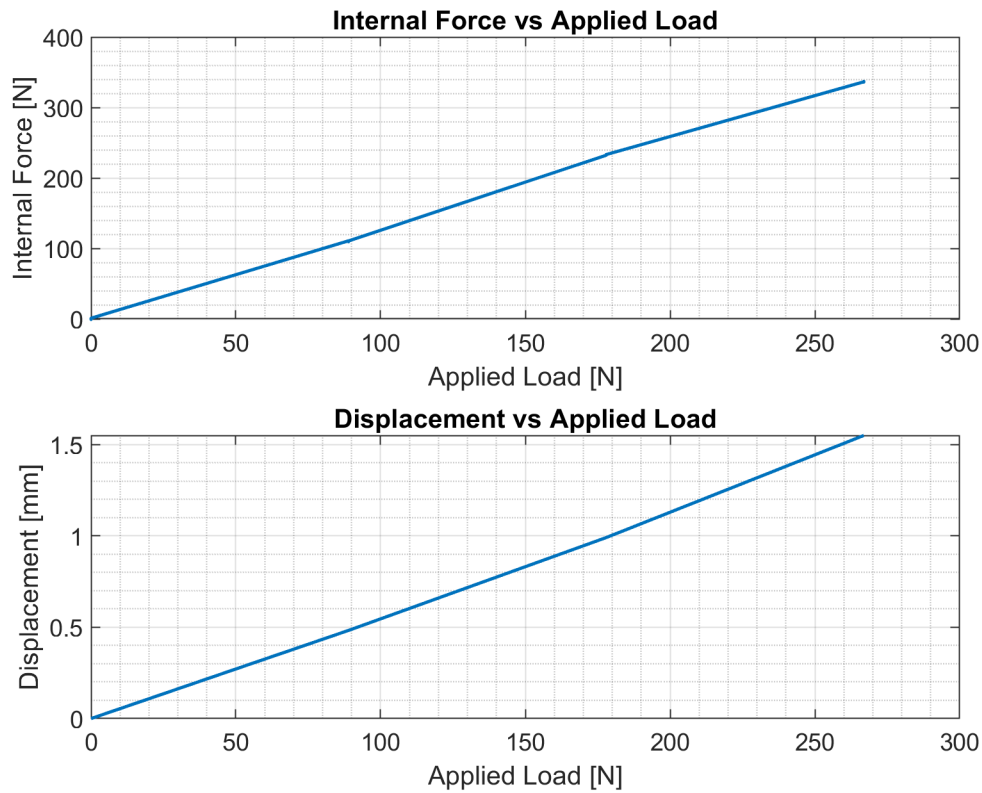


Fig. 14 Internal Force and Displacement For Loading Case 3

The second unknown loading case involved finding the location of two equal forces. This was done by treating the two forces as a single resultant force in the center of the two forces. With this, we are able to identify the midpoint between the two forces. From there, we derive the deflection each force individually. These derivations can be seen in Appendix A, titled "Case 3". Using our derived deflection equations for the left and right sides of the beam, we are able to superimpose them in order to find the deflection at the center of the truss. As opposed to the previous problem, we need to know the location and magnitude of the resultant force, that both the deflection and slope at the resultant force are equal for both the left and right beam deflection, and the constant parameters like Young's Modulus, area moment of inertia, and length of the truss. Also, the deflection at the beginning and end of the beam must be zero. These were necessary boundary conditions and constants within our derivations to solve for the constants of integration. From our experimental data, we observed the deflection at the center of the beam to be $1.549mm$. Knowing this and plugging all possible combinations of locations into MATLAB, we noticed that having a force at $0.5m$ and $3.5m$ resulted in a

deflection of 1.456mm at the center of the beam. This tells us that these locations for force one and force two are correct with approximately 6.093% error.

For this case, the experimental internal force was 266.9N where the internal force for the equivalent beam model was 341.8N . This results in an error of 28.1%. These values can be seen in Figure 14. This shows that the equivalent beam model for this case is a better approximation than it was for the previous case, but it is still not a great approximation. This could be for the same reason as discussed for the previous case. The reason why this might be a better approximation than the previous case is due to the fact that the resultant force of the two loads is closer to the center of the beam, therefore better satisfying the equivalent beam model.

IV. Discussion

A. Uncertainty Analysis

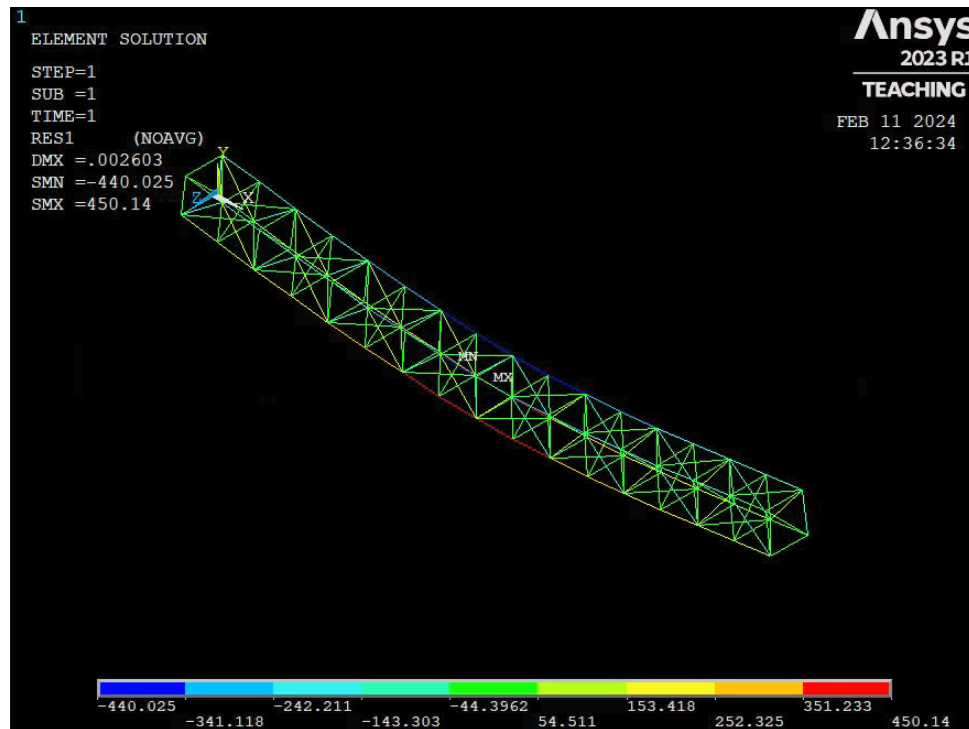


Fig. 15 Reduced Stiffness in Bars Contour Plot

The first source of error tested was reduced stiffness in the bars due to imperfect joints, such as free-play. This means that there is some degree of movement or flexibility in the bars within the truss. The ANSYS FEM analysis of this source of error can be seen in Figure 15. For this test, the Young's Modulus was set to 50GPa , down from the 70GPa that is a material feature of the 6061-T6 Aluminum bars used. While the internal forces and reaction forces were the same from loading case 1, 55.66N and 450.14N respectively, the midpoint deflection of the beam increases by 71.1% to 2.60mm . This source of error sees the largest change in midpoint deflection out of all the cases tested, making it the most important source of error. The results for all sources of error can be seen in the table below.

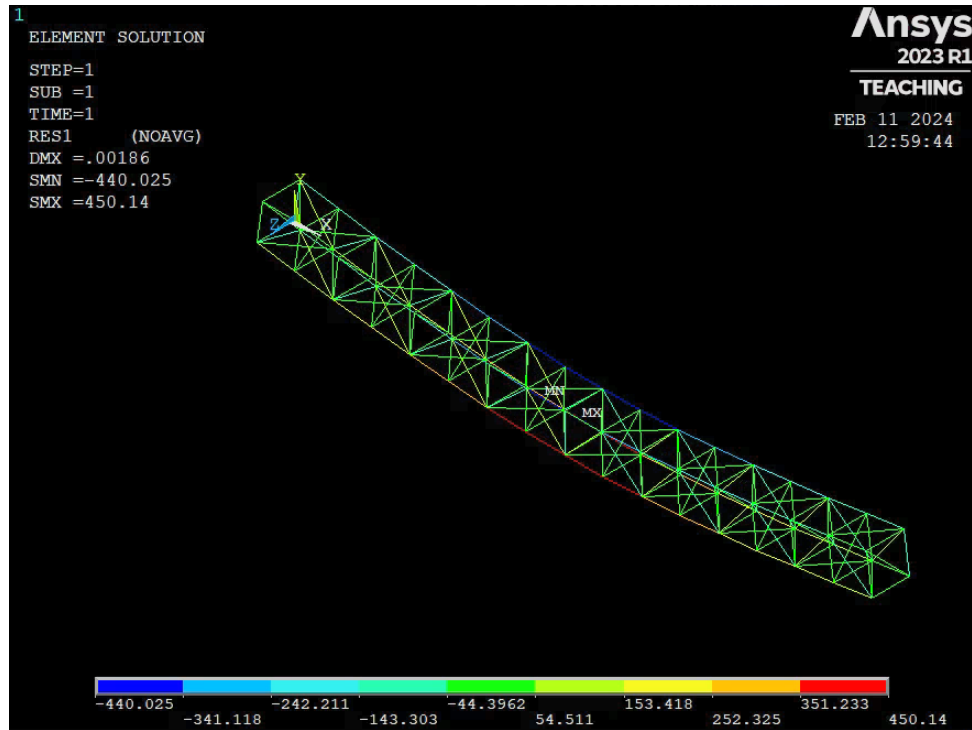


Fig. 16 Reduced Stiffness in Bar with Load Cell Contour Plot

The next source of error tested was reduced stiffness in the bar containing the load cell. This is a fair assessment of error do to the fact that the load cell introduces additional joints within the bar and is not made of 6061-T6 Aluminum. The Young's Modulus was also set to $50GPa$, but only for this one bar. The reaction forces and internal forces were identical to that of the first case. Additionally, the midpoint deflection of the beam was $1.85mm$. The original model had the same deflection, so there was no change between ANSYS models for this source of error. The most likely reason due to this is that only 1 of the 213 elements was changed, and with the model using links, the whole truss was not really affected. The contour plot for this test can be seen in Figure 16.

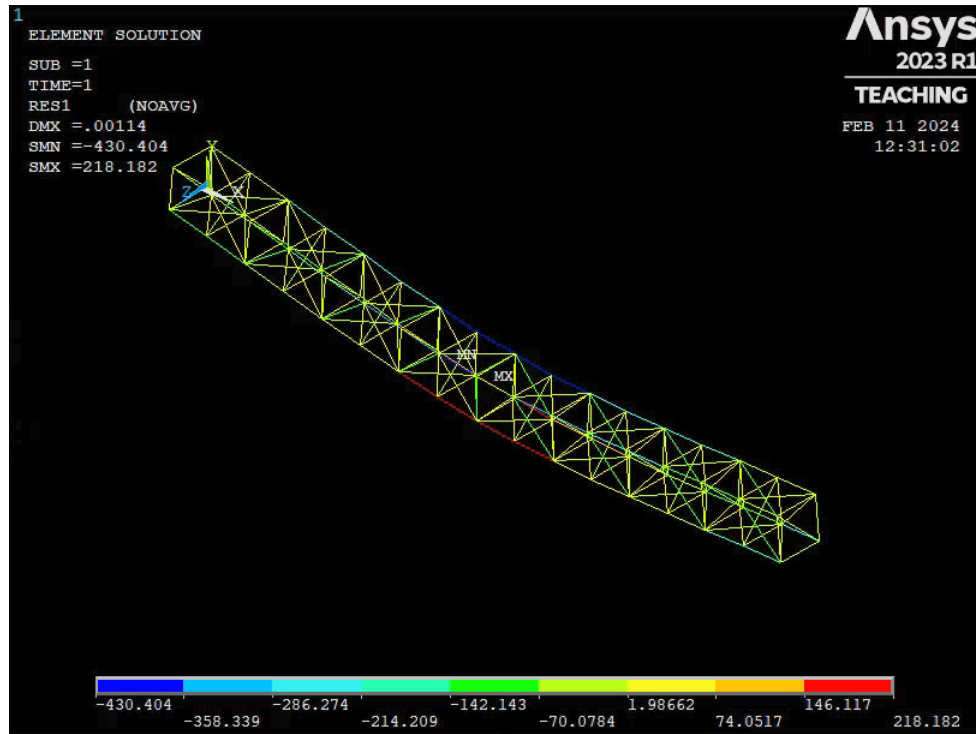


Fig. 17 Increased Friction at Joints Contour Plot

The third source of error tested was increased friction at the supported joints. Specifically, infinite friction at the joints was tested. This was modeled by assuming the roller joint was actually a pin joint, resulting in two pin joints for the truss. This test resulted in a far lower value of a maximum internal force of 229.38 N , down from 450.14 , in tension, and a slightly lower value for compression with a value of 431.19 N , down from 440.02 N . That is a 49% decrease in tension and a 2% decrease in compression. The midpoint deflection also decreased from 1.85 mm to 1.17 mm , which is a 36.75% decrease. While there is friction at the supported joints in the actual experiment, assuming that it is infinite is not necessarily an accurate assumption. While the results are interesting, it actually decreases the midpoint deflection and internal forces, which means assuming there is no friction at the roller joint is actually a better assumption than infinite friction, especially when doing the factor of safety calculation. The corresponding contour plot for this test is shown in Figure 17.

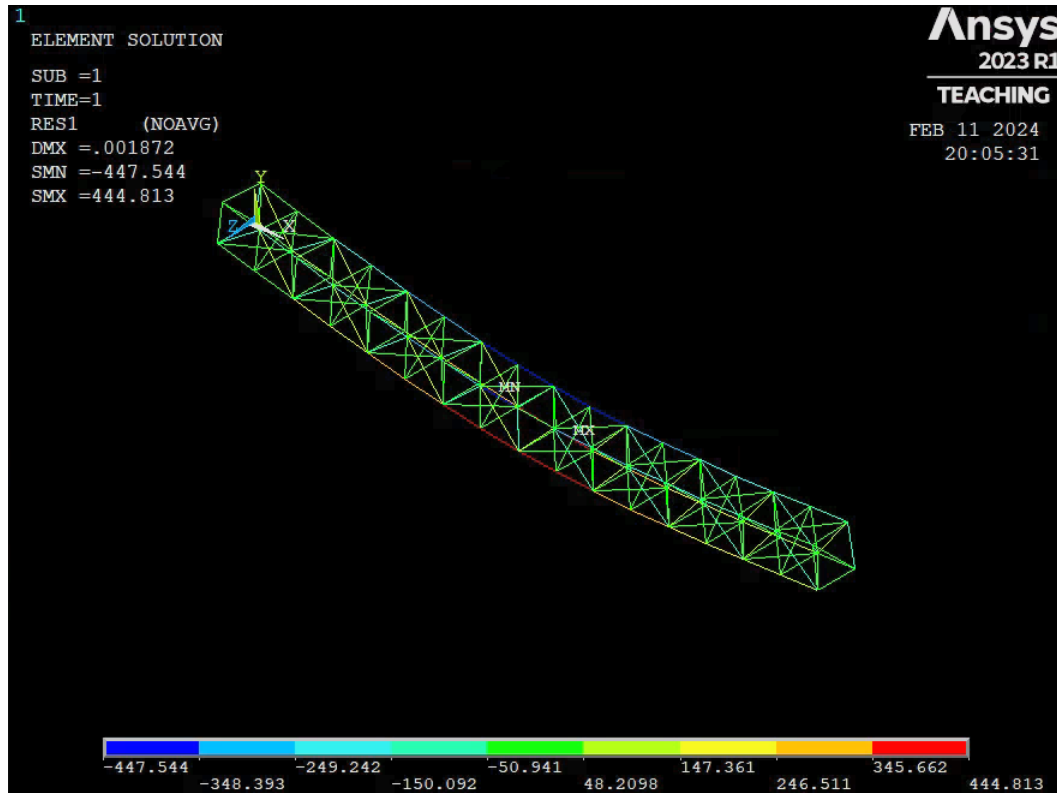


Fig. 18 Manufacturing Imperfections Contour Plot

The fourth condition tested for a possible source of error was manufacturing imperfections. To conduct this analysis, certain bars were given slightly lower and slightly higher values in length than the given value of 250mm . The range of values used was between 240mm and 260mm and the contour plot for this model can be seen in Figure 18. While this leads to slightly deformed model of the truss, the actual results do not change by a large degree, which came as a surprise. The maximum internal tension force decreased by 5.33N , the maximum internal compression force increased by 7.52N , and the midpoint deflection only increased by 0.02mm . While the change in the reaction forces was also relatively small, it was the only source of error that caused them to change by more than 1N . On the left side of the truss, nodes 1 and 52, went from 55.56N to 57.62N and 55.63N to 53.68N respectively. On the right side of the truss, nodes 17 and 68, went from 55.63N to 51.35N and 55.56N to 59.56N respectively. This is a 3% increase in node 1, 7.37% decrease in node 17, 3.18% decrease in node 52, and 7.19% increase in node 63. A range of 20mm is a pretty large range of imperfection by machined parts, so these small increases in values between models would indicate that a typical manufacturing imperfection would lead to very small sources of error.

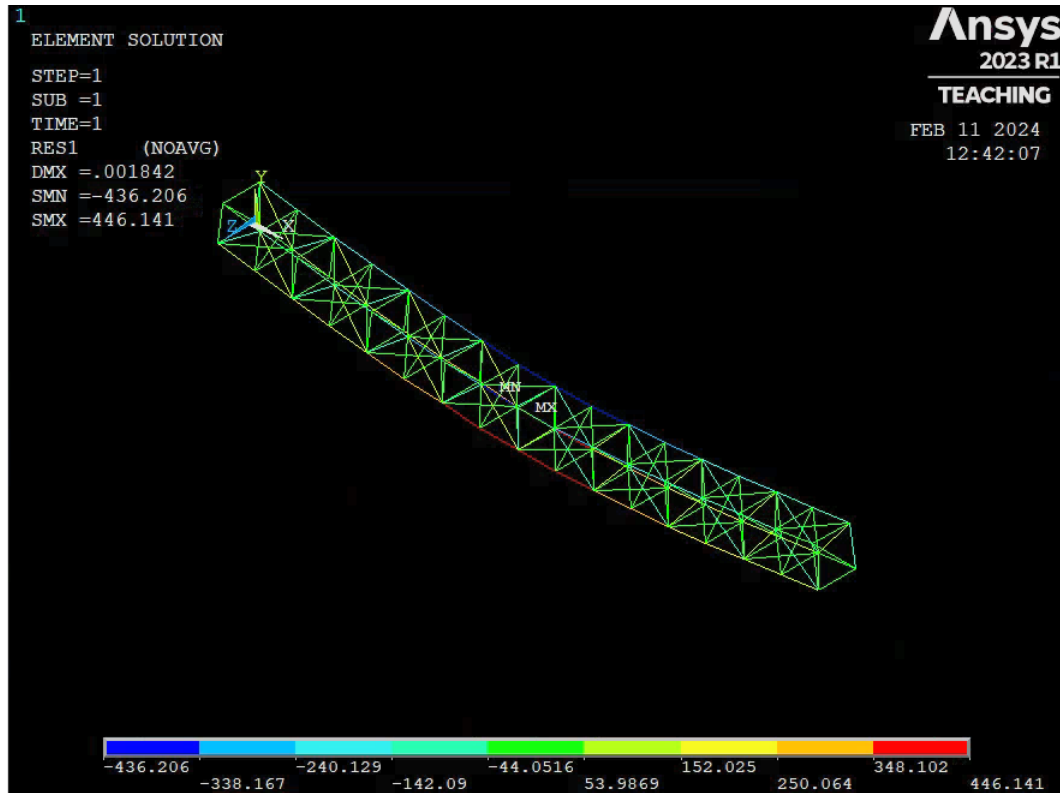


Fig. 19 Circular Tube Contour Plot

The final source of error simulated was to change the assumption that the bars act as links, and rather were the circular tubes and that the joints could transmit bending moments and the bars have bending stiffness. This was simply done by changing the cross section type in ANSYS and rerunning the simulation. Surprisingly, the change in the element type of the bar had very little to no effect on the results. The internal forces both decreased by about $4N$, the midpoint deflection decreased by $0.01mm$, and the internal forces fluctuated by $\pm 0.01N$. These minuscule changes prove that the assumption of the bars act as links instead of circular tubes is a good assumption to make for the ANSYS model. The results for this test are shown in Figure 19.

Table 6 Uncertainty Analysis of Different Test Conditions

Test Condition	Max Deflection [mm]	Max Internal Forces [N]	Reaction Forces [N]
Original Test	1.85	Tension: 450.14 Compression: 440.02	Node 1: 55.56 Node 17: 55.63 Node 52: 55.63 Node 68: 55.56
Reduced Stiffness in Bars	2.60	Tension: 450.14 Compression: 440.02	Node 1: 55.56 Node 17: 55.63 Node 52: 55.63 Node 68: 55.56
Reduced Stiffness in Bar with Load Cell	1.85	Tension: 450.14 Compression: 440.02	Node 1: 55.56 Node 17: 55.63 Node 52: 55.63 Node 68: 55.56
Increased Friction at Support Joints	1.17	Tension: 229.38 Compression: 431.19	Node 1: 55.6 Node 17: 55.6 Node 52: 55.6 Node 68: 55.6
Manufacturing Imperfections	1.87	Tension: 444.81 Compression: 447.54	Node 1: 57.62 Node 17: 51.35 Node 52: 53.86 Node 68: 59.56
Circular Tube Model	1.84	Tension: 446.14 Compression: 436.21	Node 1: 55.55 Node 17: 55.64 Node 52: 55.64 Node 68: 55.55

After modeling the 5 above sources of error in ANSYS, the most likely cause for the differences between the FEM model and the experimental results is due to increased friction at the support joints. It is the only one of the tested cases that leads to a lower maximum deflection and lower maximum internal force, which is the case for the experimental results, while keeping the reaction forces almost equal to the experimental results. While the assumption of no friction is better than the assumption of infinite friction for the FEM model, it is safe to assume there is some degree of friction at the roller joint that results in a decrease for both midpoint deflection and maximum internal force.

B. Factor of Safety

When determining the optimal factor of safety for the 16-bay truss, we assessed the uncertainty condition that resulted in the highest change in deflection. This occurred under conditions simulating reduced stiffness in bars ($E = 50GPa$). By dividing the experimental Young's Modulus by the reduced stiffness Young's Modulus, we obtained a ratio of 1.4. However, it's important to note that this approach to determining the factor of safety only considers one potential source of error. In reality, various sources of error could be present simultaneously or in combination with each other. Thus, a more comprehensive factor of safety should account for multiple sources of error within the truss system. Based on our analysis, a factor of safety ranging from 1.5 to 1.8 is considered ideal for addressing potential uncertainties effectively and is around the typical factor of safety values in the aerospace industry. If this were a part of a structure where loss of life or mission failure was a possibility if it failed, the factor of safety would scale accordingly.

V. Conclusions

The point of this lab was to analyze reaction forces, internal forces, and midpoint deflection of a truss structure through the use of three models; an experimental model, an analytical model, and an ANSYS model. By using these models we were able to predict the locations of unknown loading forces exerted on the truss. We were given experimental

data about the reaction forces and the deflection of the truss as an unknown load was applied. We were able to use the equivalent beam model to create a prediction for the locations of these loading forces. It's important to note however that when using any model, there will always be error and uncertainty. Because of this, it is important to create a factor of safety to account for the error when analyzing the exact locations of these forces. This is even more important when analyzing structures for points of failure. We explored a range of possible causes of uncertainty using the ANSYS model and derived a reasonable factor of safety based on the level of uncertainty calculated within our models.

A. Appendix

A. Complete derivations

1. Case 2/Unknown Case 1

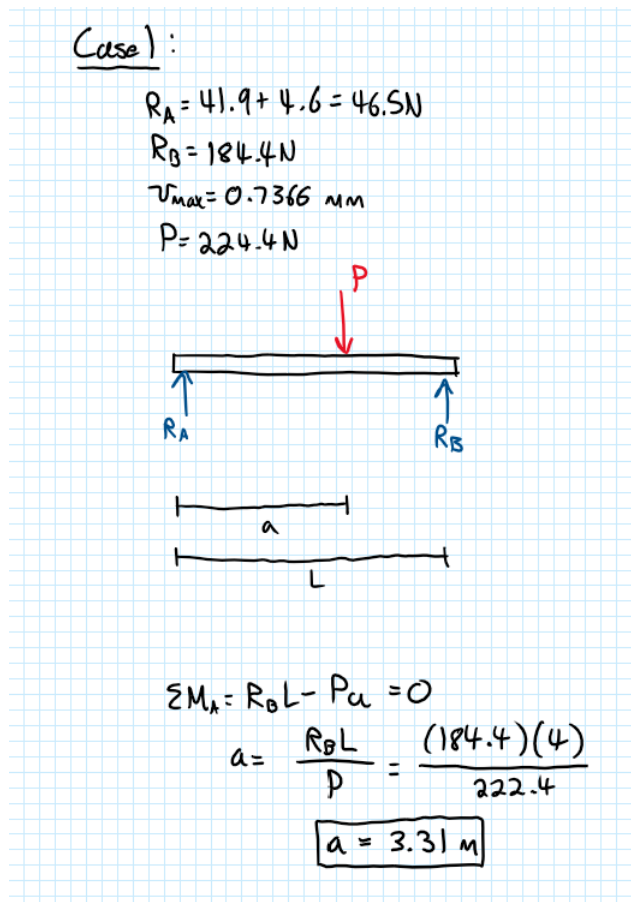
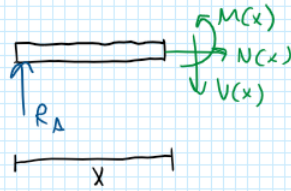


Fig. 20 Unknown Case 1 Part 1 Derivation

Solving for deflection at center:



$$\sum M_x = M(x) - R_A x = 0 \rightarrow M(x) = R_A x$$

$$\begin{aligned}\theta(x) &= \frac{1}{EI} \int M(x) dx \\ &= \frac{1}{EI} \left[\frac{R_A}{2} x^2 + C_1 \right]\end{aligned}$$

$$v(x) = \frac{1}{EI} \int \theta(x) dx$$

$$v(x) = \frac{1}{EI} \left[\frac{R_A}{6} x^3 + C_1 x + C_2 \right]$$

$$v(0) = \frac{1}{EI} C_2 = 0 \rightarrow C_2 = 0$$

$$\theta(3.25) = \frac{1}{EI} [5.281 R_A + C_1] = 0$$

$$C_1 = -5.281 R_A$$

$$v(x) = \frac{1}{EI} \left[\frac{R_A}{6} x^3 - 5.281 R_A x \right]$$

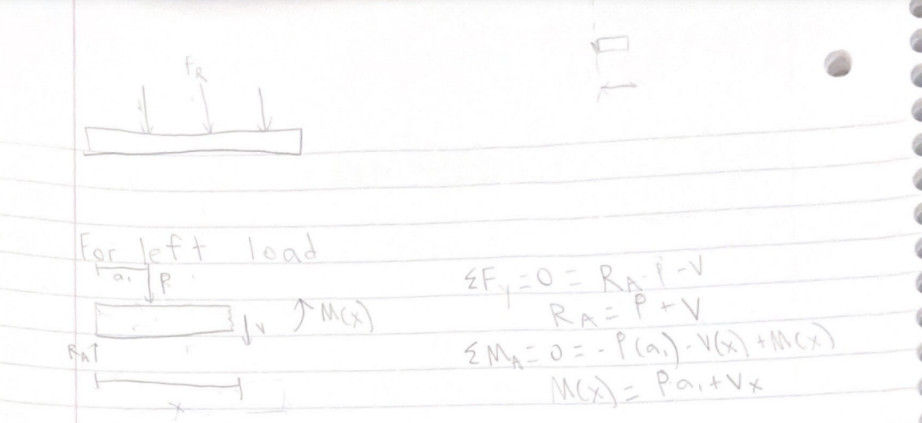
at midpoint:

$$v(2) = \frac{1}{EI} \left[\frac{R_A}{6} (2)^3 - 5.281 R_A (2) \right]$$

$$v(2) = -0.24 \text{ mm}$$

Fig. 21 Unknown Case 1 Part 2 Derivation

2. Case 3/Unknown Case 2



For left + load

$$\sum F_y = 0 = R_A - P - V$$

$$R_A = P + V$$

$$\sum M_A = 0 = -P(a_1) - V(x) + M(x)$$

$$M(x) = P a_1 + V x$$

$$V(0) = 0$$

$$M(x) = P a_1 + (R_A - P) x$$

$$V(L) = 0$$

$$\theta(L_P) = \theta_R(L_P)$$

$$V_L(L_P) = V_R(L_P)$$

$$V(x) = \frac{1}{EI} \int \int M(x) dx$$

$$\theta_R(x) = \left(P a_1 x + \frac{1}{2} (R_A - P) x^2 + C_1 \right) \frac{1}{EI}$$

$$V_R(x) = \left(\frac{P}{2} a_1 x^2 + \frac{1}{6} (R_A - P) x^3 + C_1 x + C_2 \right) \frac{1}{EI}$$

$$0 = V(L) = \frac{1}{EI} \left(\frac{P}{2} a_1 L^2 + \frac{1}{6} R_A L^3 - \frac{P}{6} L^3 + C_1 L + C_2 \right)$$

$$C_2 = -\frac{P}{2} a_1 L^2 - \frac{1}{6} R_A L^3 + \frac{P}{6} L^3 - C_1 L$$

$$V(x) = \frac{1}{EI} \left(\frac{P}{2} a_1 x^2 + \frac{1}{6} (R_A - P) x^3 - \frac{P}{2} a_1 L^2 - \frac{1}{6} R_A L^3 + \frac{P}{6} L^3 + C_1 (x - L) \right)$$

$$V(L_P) = \frac{1}{EI} \left(\frac{P}{2} a_1 L_P^2 + \frac{1}{6} (R_A - P) L_P^3 - \frac{P}{2} a_1 L^2 - \frac{1}{6} R_A L^3 + \frac{P}{6} L^3 + C_1 (L_P - L) \right)$$

Fig. 22 Unknown Case 2 Part 1 Derivation

For right load $\sum F_y = 0 = R_A - V$
 $R_A = V$
 $\sum M_A = 0 = -Vx + M(x)$
 $M(x) = Vx$

$V_L(x) = \frac{1}{EI} \int M(x) dx$
 $\theta_L(x) = \frac{1}{EI} \left(\frac{1}{2} P_0 x^2 + C_3 \right)$
 $\theta_L(L_P) = \frac{1}{EI} \left(\frac{1}{2} P_0 L_P^2 + C_3 \right)$
 $V_L(x) = \frac{1}{EI} \left(\frac{1}{6} V x^3 + C_3 x + C_4 \right)$
 $C_4 = -\frac{1}{6} R_A L^3 + C_3 L$

$V_L(x) = \frac{1}{EI} \left(\frac{1}{6} R_A x^3 + C_3 x + C_4 \right)$
 $V_L(L_P) = \frac{1}{EI} \left(\frac{1}{6} R_A L_P^3 + C_3 L_P + C_4 \right)$

Fig. 23 Unknown Case 2 Part 2 Derivation

$V_L(L_P) = V_R(L_P)$
 $\frac{1}{6} R_A L_P^3 + C_3 L_P = \frac{P}{2} \alpha_1 L_P^2 + \frac{1}{6} R_A L_P^3 - \frac{1}{6} P L_P^3 - \frac{P}{2} \alpha_1 L^2 - \frac{1}{6} R_A L^3$
 $+ \frac{P}{6} L^3 + C_1 (L_P - L)$
 $C_3 L_P = \frac{P}{2} \alpha_1 L_P - \frac{1}{6} P L_P^3 - \frac{P}{2} \alpha_1 L^2 - \frac{1}{6} R_A L^3 + \frac{P}{6} L^3 + C_1 (L_P - L)$
 $C_3 = \frac{P}{2} \alpha_1 - \frac{1}{6} P L_P^2 + \left(\frac{1}{L_P} \right) \left(-\frac{P}{2} \alpha_1 L^2 - \frac{1}{6} R_A L^3 + \frac{P}{6} L^3 + C_1 (L_P - L) \right)$

Fig. 24 Unknown Case 2 Part 3 Derivation

$\theta_R(L_P) = \theta_L(L_P)$
 $P \alpha_1 L_P + \frac{1}{2} R_A L_P^2 - \frac{P}{2} L_P^2 + C_1 = \frac{1}{2} R_A L_P^2 + C_3$
 $P \alpha_1 L_P - \frac{P}{2} L_P^2 + C_1 = C_3$
 $C_1 = C_3 - P \alpha_1 L_P + \frac{P}{2} L_P^2$
 $C_1 (L_P - L) = \left(\frac{1}{3} L_P - C_3 L^3 - P \alpha_1 L_P^2 + P \alpha_1 L_P L + \frac{P}{2} L_P^3 - \frac{P}{2} L_P^2 L \right)$
 $C_3 - C_3 L_P + C_3 L = C_3 (1 - L_P + L)$
 $C_3 = \frac{P}{2} \alpha_1 - \frac{1}{6} P L_P^2 + \left(\frac{1}{L_P} \right) \left(-\frac{P}{2} \alpha_1 L^2 - \frac{1}{6} R_A L^3 + \frac{P}{6} L^3 - P \alpha_1 L_P^2 + P \alpha_1 L_P L + \frac{P}{2} L_P^3 - \frac{P}{2} L_P^2 L \right)$
 $(1 - L_P + L)$

Fig. 25 Unknown Case 2 Part 4 Derivation

B. Matlab Code

```
1 %% House Keeping
2 clear,clc,close all
3
4 %% Read In Data
5 case_1_data = readmatrix("Case 1.txt");
6 case_2_data = readmatrix("Case 2.txt");
7 case_3_data = readmatrix("Case 3.txt");
8
9 case_1_data = case_1_data * 4.4482216153;
10 case_2_data = case_2_data * 4.4482216153;
11 case_3_data = case_3_data * 4.4482216153;
12
13
14 %% Sort Data
15
16 % Applied force for each case
17 case_1_applied_force = case_1_data(:,1);
18 case_2_applied_force = case_2_data(:,1);
19 case_3_applied_force = case_3_data(:,1);
20
21 % Reaction forces for each case
22 case_1_load_sensor_1 = case_1_data(:,2); % Case 1
23 case_1_load_sensor_2 = case_1_data(:,3);
24 case_1_load_sensor_3 = case_1_data(:,4);
25
26 case_2_load_sensor_1 = case_2_data(:,2); % Case 2
27 case_2_load_sensor_2 = case_2_data(:,3);
28 case_2_load_sensor_3 = case_2_data(:,4);
29
30 case_3_load_sensor_1 = case_3_data(:,2); % Case 3
31 case_3_load_sensor_2 = case_3_data(:,3);
32 case_3_load_sensor_3 = case_3_data(:,4);
33
34 % Internal force for each case
35 case_1_inline_load_cells = case_1_data(:,5) - mean(case_1_data(1:10,5));
36 case_2_inline_load_cells = case_2_data(:,5) - mean(case_2_data(1:10,5));
37 case_3_inline_load_cells = case_3_data(:,5) - mean(case_3_data(1:10,5));
38
39 % Displacement for each case
40 case_1_LVDT = (case_1_data(:,6)./4.4482216153)*25.4;
41 case_2_LVDT = (case_2_data(:,6)./4.4482216153)*25.4;
42 case_3_LVDT = (case_3_data(:,6)./4.4482216153)*25.4;
43
44 %% Finding Loading Location
45
46 % Both cases assume that loading sensor 3 = Rb
47 % Case 2
48 L = 4;
49 a1 = (L.*case_2_load_sensor_3)./case_2_applied_force;
50
51 % Case 3
52 a2 = (L.*case_3_load_sensor_3)./case_3_applied_force;
53
54 E = 70E9;
55 I = 2.4761E-6;
56 RA = max(case_3_load_sensor_1 + case_3_load_sensor_2);
57 RB = max(case_3_load_sensor_3);
```



```

58 P = (RA+RB)/2;
59 L = 4;
60 Lp = 2;
61 a = 0:.25:2;
62 % a3 = 0.08:0.01:2.04;
63 % a4 = 4:-0.01:2.04;
64 %
65 % v_left = 1/(E*I) .* ((RA/6)*x^3 - (RA/2) .* a3.^2.*x);
66 % v_right = 1/(E*I) .* ((RA/6 -
    P/12)*x^3+(P/4).*a3.*x^2+((P/4).*a4.^2-(P/2).*a3.*a4-(RA/2).*a4.^2).*x);
67 % v_left = v_left .* 1000;
68 % v_right = v_right .* 1000;
69 %
70 % v_tot = v_left + v_right;
71 %
72 v_c = max(case_3_LVDT);
73
74 C3 = ((P/2).*a - (1/6)*P*(Lp^2)+(1/Lp).*((-P/2).*a.*(L.^2) -
    (1/6)*RA*(L^3)+(P/6)*(L^3)-P.*a.*(Lp.^2)+P.*a.*L.*Lp+(P/2)*Lp^3-(P/2)*(Lp^2)*L))./(1-Lp+L);
75 C1 = C3 -P.*a.*Lp+(P/2)*Lp;
76 C2 = (-P/2).*a.*L.^2 - (1/6)*RA*L^3+(P/6)*L^3-C1.*L;
77
78 v_r = (1/(E*I)).*((P/2).*a.*Lp^2 + (1/6)*(RA-P)*(Lp^3)+C1*Lp+C2);
79 v_l = (1/(E*I)).*((1/6)*RA*(Lp^3)+C3*Lp);
80
81 v_tot = v_l + v_r;
82
83 location1 = a(3); %m
84 location2 = (L - location1); %m
85
86 errorv = abs((-v_tot(3)*1000 - v_c)/v_c) *100;
87
88
89 %% Linear Regression
90
91 % Case 1
92 P_R1_1 = polyfit(case_1_applied_force, case_1_load_sensor_1, 1);
93 P_R2_1 = polyfit(case_1_applied_force, case_1_load_sensor_2, 1);
94 P_R3_1 = polyfit(case_1_applied_force, case_1_load_sensor_3, 1);
95 P_I_1 = polyfit(case_1_applied_force, case_1_inline_load_cells, 1);
96 P_D_1 = polyfit(case_1_applied_force, case_1_LVDT, 1);
97
98 fit_R1_1 = polyval(P_R1_1, case_1_applied_force);
99 fit_R2_1 = polyval(P_R2_1, case_1_applied_force);
100 fit_R3_1 = polyval(P_R3_1, case_1_applied_force);
101 fit_I_1 = polyval(P_I_1, case_1_applied_force);
102 fit_D_1 = polyval(P_D_1, case_1_applied_force);
103
104 % Case 2
105 P_R1_2 = polyfit(case_2_applied_force, case_2_load_sensor_1, 1);
106 P_R2_2 = polyfit(case_2_applied_force, case_2_load_sensor_2, 1);
107 P_R3_2 = polyfit(case_2_applied_force, case_2_load_sensor_3, 1);
108 P_I_2 = polyfit(case_2_applied_force, case_2_inline_load_cells, 1);
109 P_D_2 = polyfit(case_2_applied_force, case_2_LVDT, 1);
110
111 fit_R1_2 = polyval(P_R1_2, case_2_applied_force);
112 fit_R2_2 = polyval(P_R2_2, case_2_applied_force);
113 fit_R3_2 = polyval(P_R3_2, case_2_applied_force);
114 fit_I_2 = polyval(P_I_2, case_2_applied_force);

```

```

115 fit_D_2 = polyval(P_D_2, case_2_applied_force);
116
117 % Case 3
118 P_R1_3 = polyfit(case_3_applied_force, case_3_load_sensor_1, 1);
119 P_R2_3 = polyfit(case_3_applied_force, case_3_load_sensor_2, 1);
120 P_R3_3 = polyfit(case_3_applied_force, case_3_load_sensor_3, 1);
121 P_I_3 = polyfit(case_3_applied_force, case_3_inline_load_cells, 1);
122 P_D_3 = polyfit(case_3_applied_force, case_3_LVDT, 1);
123
124 fit_R1_3 = polyval(P_R1_3, case_3_applied_force);
125 fit_R2_3 = polyval(P_R2_3, case_3_applied_force);
126 fit_R3_3 = polyval(P_R3_3, case_3_applied_force);
127 fit_I_3 = polyval(P_I_3, case_3_applied_force);
128 fit_D_3 = polyval(P_D_3, case_3_applied_force);
129
130 %% Standard Deviation of the forces
131 N = 110; %The number of measurements taken
132
133 %Reaction Force #1
134 sigma_force_R1_1 = ((1)/(N-1)) .* (mean(case_1_load_sensor_1) - case_1_load_sensor_1).^2;
135 sigma_force_R1_C1 = sqrt(sigma_force_R1_1);
136
137 sigma_force_R1_2 = ((1)/(N-1)) .* (mean(case_1_load_sensor_2) - case_1_load_sensor_2).^2;
138 sigma_force_R1_C2 = sqrt(sigma_force_R1_2);
139
140 sigma_force_R1_3 = ((1)/(N-1)) .* (mean(case_1_load_sensor_3) - case_1_load_sensor_3).^2;
141 sigma_force_R1_C3 = sqrt(sigma_force_R1_3);
142
143
144 %Reaction Force #2
145 sigma_force_R2_1 = ((1)/(N-1)) .* (mean(case_2_load_sensor_1) - case_2_load_sensor_1).^2;
146 sigma_force_R2_C1 = sqrt(sigma_force_R2_1);
147
148 sigma_force_R2_2 = ((1)/(N-1)) .* (mean(case_2_load_sensor_2) - case_2_load_sensor_2).^2;
149 sigma_force_R2_C2 = sqrt(sigma_force_R2_2);
150
151 sigma_force_R2_3 = ((1)/(N-1)) .* (mean(case_2_load_sensor_3) - case_2_load_sensor_3).^2;
152 sigma_force_R2_C3 = sqrt(sigma_force_R2_3);
153
154 %Reaction Force #3
155 sigma_force_R3_1 = ((1)/(N-1)) .* (mean(case_3_load_sensor_1) - case_3_load_sensor_1).^2;
156 sigma_force_R3_C1 = sqrt(sigma_force_R3_1);
157
158 N3 = 70;
159 sigma_force_R3_2 = ((1)/(N3-1)) .* (mean(case_3_load_sensor_2) - case_3_load_sensor_2).^2;
160 sigma_force_R3_C2 = sqrt(sigma_force_R3_2);
161
162 sigma_force_R3_3 = ((1)/(N-1)) .* (mean(case_3_load_sensor_3) - case_3_load_sensor_3).^2;
163 sigma_force_R3_C3 = sqrt(sigma_force_R3_3);
164
165 %Internal Forces
166 Sigma_internal_force_1 = ((1)/(N-1)) .* (mean(case_1_inline_load_cells) -
    case_1_inline_load_cells).^2;
167 Sigma_internal_force_C1 = sqrt(Sigma_internal_force_1);
168
169 Sigma_internal_force_2 = ((1)/(N-1)) .* (mean(case_2_inline_load_cells) -
    case_2_inline_load_cells).^2;
170 Sigma_internal_force_C2 = sqrt(Sigma_internal_force_2);
171

```

```

172 Sigma_internal_force_3 = ((1)/(N-1)) .* (mean(case_3_inline_load_cells) -
    case_3_inline_load_cells).^2;
173 Sigma_internal_force_C3 = sqrt(Sigma_internal_force_3);
174
175 %Displacement
176 Sigma_displacement_1 = ((1)/(N-1)) .* (mean(case_1_LVDT) - case_1_LVDT).^2;
177 Sigma_displacement_C1 = sqrt(Sigma_displacement_1);
178
179 Sigma_displacement_2 = ((1)/(N-1)) .* (mean(case_2_LVDT) - case_2_LVDT).^2;
180 Sigma_displacement_C2 = sqrt(Sigma_displacement_2);
181
182 Sigma_displacement_3 = ((1)/(N3-1)) .* (mean(case_3_LVDT) - case_3_LVDT).^2;
183 Sigma_displacement_C3 = sqrt(Sigma_displacement_3);
184
185
186 %% Uncertainty Analysis
187
188
189 %% R^2
190
191 % SSR Values
192 SSR_R1_1 = 0; % Case 1
193 SSR_R2_1 = 0;
194 SSR_R3_1 = 0;
195 SSR_I_1 = 0;
196 SSR_D_1 = 0;
197
198 SSR_R1_2 = 0; % Case 2
199 SSR_R2_2 = 0;
200 SSR_R3_2 = 0;
201 SSR_I_2 = 0;
202 SSR_D_2 = 0;
203
204 SSR_R1_3 = 0; % Case 3
205 SSR_R2_3 = 0;
206 SSR_R3_3 = 0;
207 SSR_I_3 = 0;
208 SSR_D_3 = 0;
209
210 % Find sum of the residuals
211 for i = 1:length(case_1_load_sensor_1) % Case 1 and 2
212
213     SSR_R1_1 = SSR_R1_1 + ((case_1_load_sensor_1(i) - fit_R1_1(i)).^2);
214     SSR_R2_1 = SSR_R2_1 + ((case_1_load_sensor_2(i) - fit_R2_1(i)).^2);
215     SSR_R3_1 = SSR_R3_1 + ((case_1_load_sensor_3(i) - fit_R3_1(i)).^2);
216     SSR_I_1 = SSR_I_1 + ((case_1_inline_load_cells(i) - fit_I_1(i)).^2);
217     SSR_D_1 = SSR_D_1 + ((case_1_LVDT(i) - fit_D_1(i)).^2);
218
219     SSR_R1_2 = SSR_R1_2 + ((case_2_load_sensor_1(i) - fit_R1_2(i)).^2);
220     SSR_R2_2 = SSR_R2_2 + ((case_2_load_sensor_2(i) - fit_R2_2(i)).^2);
221     SSR_R3_2 = SSR_R3_2 + ((case_2_load_sensor_3(i) - fit_R3_2(i)).^2);
222     SSR_I_2 = SSR_I_2 + ((case_2_inline_load_cells(i) - fit_I_2(i)).^2);
223     SSR_D_2 = SSR_D_2 + ((case_2_LVDT(i) - fit_D_2(i)).^2);
224
225 end
226
227 for i = 1:length(case_3_load_sensor_1) % Case 3
228
229     SSR_R1_3 = SSR_R1_3 + ((case_3_load_sensor_1(i) - fit_R1_3(i)).^2);

```

```

230     SSR_R2_3 = SSR_R2_3 + ((case_3_load_sensor_2(i) - fit_R2_3(i)).^2);
231     SSR_R3_3 = SSR_R3_3 + ((case_3_load_sensor_3(i) - fit_R3_3(i)).^2);
232     SSR_I_3 = SSR_I_3 + ((case_3_inline_load_cells(i) - fit_I_3(i)).^2);
233     SSR_D_3 = SSR_D_3 + ((case_3_LVDT(i) - fit_D_3(i)).^2);
234 end
235
236 % SST values
237 SST_R1_1 = 0; % Case 1
238 SST_R2_1 = 0;
239 SST_R3_1 = 0;
240 SST_I_1 = 0;
241 SST_D_1 = 0;
242
243 SST_R1_2 = 0; % Case 2
244 SST_R2_2 = 0;
245 SST_R3_2 = 0;
246 SST_I_2 = 0;
247 SST_D_2 = 0;
248
249 SST_R1_3 = 0; % Case 3
250 SST_R2_3 = 0;
251 SST_R3_3 = 0;
252 SST_I_3 = 0;
253 SST_D_3 = 0;
254
255 % Mean values
256 M_R1_1 = mean(case_1_load_sensor_1); % Case 1
257 M_R2_1 = mean(case_1_load_sensor_2);
258 M_R3_1 = mean(case_1_load_sensor_3);
259 M_I_1 = mean(case_1_inline_load_cells);
260 M_D_1 = mean(case_1_LVDT);
261
262 M_R1_2 = mean(case_2_load_sensor_1); % Case 2
263 M_R2_2 = mean(case_2_load_sensor_2);
264 M_R3_2 = mean(case_2_load_sensor_3);
265 M_I_2 = mean(case_2_inline_load_cells);
266 M_D_2 = mean(case_2_LVDT);
267
268 M_R1_3 = mean(case_3_load_sensor_1); % Case 3
269 M_R2_3 = mean(case_3_load_sensor_2);
270 M_R3_3 = mean(case_3_load_sensor_3);
271 M_I_3 = mean(case_3_inline_load_cells);
272 M_D_3 = mean(case_3_LVDT);
273
274 % Finding SST Values
275 for i = 1:length(case_1_load_sensor_1) % Case 1 and 2
276
277     SST_R1_1 = SST_R1_1 + ((case_1_load_sensor_1(i) - M_R1_1).^2);
278     SST_R2_1 = SST_R2_1 + ((case_1_load_sensor_2(i) - M_R2_1).^2);
279     SST_R3_1 = SST_R3_1 + ((case_1_load_sensor_3(i) - M_R3_1).^2);
280     SST_I_1 = SST_I_1 + ((case_1_inline_load_cells(i) - M_I_1).^2);
281     SST_D_1 = SST_D_1 + ((case_1_LVDT(i) - M_D_1).^2);
282
283     SST_R1_2 = SST_R1_2 + ((case_2_load_sensor_1(i) - M_R1_2).^2);
284     SST_R2_2 = SST_R2_2 + ((case_2_load_sensor_2(i) - M_R2_2).^2);
285     SST_R3_2 = SST_R3_2 + ((case_2_load_sensor_3(i) - M_R3_2).^2);
286     SST_I_2 = SST_I_2 + ((case_2_inline_load_cells(i) - M_I_2).^2);
287     SST_D_2 = SST_D_2 + ((case_2_LVDT(i) - M_D_2).^2);
288

```

```

289 end
290
291 for i = 1:length(case_3_load_sensor_1) % Case 3
292
293     SST_R1_3 = SST_R1_3 + ((case_3_load_sensor_1(i) - M_R1_3).^2);
294     SST_R2_3 = SST_R2_3 + ((case_3_load_sensor_2(i) - M_R2_3).^2);
295     SST_R3_3 = SST_R3_3 + ((case_3_load_sensor_3(i) - M_R3_3).^2);
296     SST_I_3 = SST_I_3 + ((case_3_inline_load_cells(i) - M_I_3).^2);
297     SST_D_3 = SST_D_3 + ((case_3_LVDT(i) - M_D_3).^2);
298
299 end
300
301 % Finding R^2 Values
302 case_1_R_Squared(1) = 1 - (SSR_R1_1./SST_R1_1); % Case 1
303 case_1_R_Squared(2) = 1 - (SSR_R2_1./SST_R2_1);
304 case_1_R_Squared(3) = 1 - (SSR_R3_1./SST_R3_1);
305 case_1_R_Squared(4) = 1 - (SSR_I_1./SST_I_1);
306 case_1_R_Squared(5) = 1 - (SSR_D_1./SST_D_1);
307
308 case_2_R_Squared(1) = 1 - (SSR_R1_2./SST_R1_2); % Case 2
309 case_2_R_Squared(2) = 1 - (SSR_R2_2./SST_R2_2);
310 case_2_R_Squared(3) = 1 - (SSR_R3_2./SST_R3_2);
311 case_2_R_Squared(4) = 1 - (SSR_I_2./SST_I_2);
312 case_2_R_Squared(5) = 1 - (SSR_D_2./SST_D_2);
313
314 case_3_R_Squared(1) = 1 - (SSR_R1_3./SST_R1_3); % Case 3
315 case_3_R_Squared(2) = 1 - (SSR_R2_3./SST_R2_3);
316 case_3_R_Squared(3) = 1 - (SSR_R3_3./SST_R3_3);
317 case_3_R_Squared(4) = 1 - (SSR_I_3./SST_I_3);
318 case_3_R_Squared(5) = 1 - (SSR_D_3./SST_D_3);
319
320
321 %% Plots
322
323 figure(1) % Reaction Force 1
324 hold on
325
326 %scatter(case_1_applied_force, case_1_load_sensor_1,"LineWidth", 1.2) %Blue
327 errorbar(case_1_applied_force,case_1_load_sensor_1,ones(size(sigma_force_R1_C1)))
328 %scatter(case_2_applied_force, case_2_load_sensor_1,"LineWidth", 1.2) %Red
329 errorbar(case_2_applied_force,case_2_load_sensor_1,sigma_force_R2_C1)
330 %scatter(case_3_applied_force, case_3_load_sensor_1,"LineWidth", 1.2) %Yellow
331 errorbar(case_3_applied_force,case_3_load_sensor_1,sigma_force_R3_C1)
332
333 plot(case_1_applied_force, fit_R1_1,"LineWidth", 1.2, "Color", [0 0.4470 0.7410])
334 plot(case_2_applied_force, fit_R1_2,"LineWidth", 1.2, "Color", [0.8500 0.3250 0.0980])
335 plot(case_3_applied_force, fit_R1_3,"LineWidth", 1.2, "Color", [0.9290 0.6940 0.1250])
336
337
338 xlabel("Applied Force (N)")
339 ylabel("Measured Reaction Force (N)")
340 title("Reaction Force 1 vs Applied Force")
341 legend('Case 1', 'Case 2', 'Case 3')
342 hold off
343
344
345
346 figure(2) % Reaction Force 2
347 hold on

```

```

348
349 %scatter(case_1_applied_force, case_1_load_sensor_2,"LineWidth", 1.2)
350 errorbar(case_1_applied_force,case_1_load_sensor_2,ones(size(sigma_force_R1_C2)))
351 %errorbar(case_1_applied_force,case_1_load_sensor_2,sigma_force_R3_C3)
352 %scatter(case_2_applied_force, case_2_load_sensor_2,"LineWidth", 1.2)
353 errorbar(case_2_applied_force,case_2_load_sensor_2,ones(size(sigma_force_R2_C2)))
354 %scatter(case_3_applied_force, case_3_load_sensor_2,"LineWidth", 1.2)
355 errorbar(case_3_applied_force,case_3_load_sensor_2,ones(size(sigma_force_R3_C2)))
356
357 plot(case_1_applied_force, fit_R2_1,"LineWidth", 1.2, "Color", [0 0.4470 0.7410])
358 plot(case_2_applied_force, fit_R2_2,"LineWidth", 1.2, "Color", [0.8500 0.3250 0.0980])
359 plot(case_3_applied_force, fit_R2_3,"LineWidth", 1.2, "Color", [0.9290 0.6940 0.1250])
360
361 xlabel("Applied Force (N)")
362 ylabel("Measured Reaction Force (N)")
363 title("Reaction Force 2 vs Applied Force")
364 legend('Case 1', 'Case 2', 'Case 3')
365 hold off
366
367 figure(3) % Reaction Force 3
368
369 hold on
370 %scatter(case_1_applied_force, case_1_load_sensor_3,"LineWidth",1.2)
371 errorbar(case_1_applied_force,case_1_load_sensor_3,ones(size(sigma_force_R1_C3)))
372 %scatter(case_2_applied_force, case_2_load_sensor_3,"LineWidth", 1.2)
373 errorbar(case_2_applied_force,case_2_load_sensor_3,ones(size(sigma_force_R2_C3)))
374 %scatter(case_3_applied_force, case_3_load_sensor_3,"LineWidth", 1.2)
375 errorbar(case_3_applied_force,case_3_load_sensor_3,ones(size(sigma_force_R3_C3)))
376
377 plot(case_1_applied_force, fit_R3_1,"LineWidth", 1.2, "Color", [0 0.4470 0.7410])
378 plot(case_2_applied_force, fit_R3_2,"LineWidth", 1.2, "Color", [0.8500 0.3250 0.0980])
379 plot(case_3_applied_force, fit_R3_3,"LineWidth", 1.2, "Color", [0.9290 0.6940 0.1250])
380
381 xlabel("Applied Force (N)")
382 ylabel("Measured Reaction Force (N)")
383 title("Reaction Force 3 vs Applied Force")
384 legend('Case 1', 'Case 2', 'Case 3')
385 hold off
386
387 figure(4) % Internal Force
388
389 hold on
390 %scatter(case_1_applied_force, case_1_inline_load_cells,"LineWidth", 1.2)
391 errorbar(case_1_applied_force,case_1_inline_load_cells,ones(size(Sigma_internal_force_C1)))
392 %scatter(case_2_applied_force, case_2_inline_load_cells,"LineWidth", 1.2)
393 errorbar(case_2_applied_force,case_2_inline_load_cells,ones(size(Sigma_internal_force_C2)))
394 %scatter(case_3_applied_force, case_3_inline_load_cells,"LineWidth", 1.2)
395 errorbar(case_3_applied_force,case_3_inline_load_cells,ones(size(Sigma_internal_force_C3)))
396
397 plot(case_1_applied_force, fit_I_1,"LineWidth", 1.2, "Color", [0 0.4470 0.7410])
398 plot(case_2_applied_force, fit_I_2,"LineWidth", 1.2, "Color", [0.8500 0.3250 0.0980])
399 plot(case_3_applied_force, fit_I_3,"LineWidth", 1.2, "Color", [0.9290 0.6940 0.1250])
400
401 xlabel("Applied Force (N)")
402 ylabel("Measured Internal Force (N)")
403 title("Internal Force vs Applied Force")
404 legend('Case 1', 'Case 2', 'Case 3')
405 hold off
406

```

```

407 figure(5) % Displacement
408
409 hold on
410 scatter(case_1_applied_force, case_1_LVDT,"LineWidth", 1.2)
411 %errorbar(case_1_applied_force,case_1_LVDT,ones(size(Sigma_displacement_C1)))
412 scatter(case_2_applied_force, case_2_LVDT,"LineWidth", 1.2)
413 %errorbar(case_2_applied_force,case_2_LVDT,ones(size(Sigma_displacement_C2)))
414 scatter(case_3_applied_force, case_3_LVDT,"LineWidth", 1.2)
415 %errorbar(case_3_applied_force,case_3_LVDT,ones(size(Sigma_displacement_C3)))
416 % xlim([0 300])
417 % ylim([-0.2 1.6])
418
419 plot(case_1_applied_force, fit_D_1,"LineWidth", 1.2, "Color", [0 0.4470 0.7410])
420 plot(case_2_applied_force, fit_D_2,"LineWidth", 1.2, "Color", [0.8500 0.3250 0.0980])
421 plot(case_3_applied_force, fit_D_3,"LineWidth", 1.2, "Color", [0.9290 0.6940 0.1250])
422
423 xlabel("Applied Force (N)")
424 ylabel("Measured Mid-Point Displacement (mm)")
425 title("Measured Mid-Point Displacement vs Applied Force")
426 legend('Case 1', 'Case 2', 'Case 3')
427 hold off
428
429 %% Plots Question 2
430
431 P1 = 0:44.48:222.4;
432 x = 2;
433 % Reaction Force 1
434
435 figure(6)
436 subplot(3,1,1)
437 title('Reactions Forces at F0')
438 hold on
439 plot(case_1_applied_force, fit_R1_1,"LineWidth", 1.2, "Color", [0 0.4470 0.7410])
440 grid on; grid minor
441 plot(P1,P1/4)
442 plot(222.4,55.56,'ok')
443 xlabel('Applied Force [N]')
444 ylabel('F0 Reaction Force [N]')
445 hold off
446 subplot(3,1,2)
447 title('Reactions Forces at F1')
448 hold on
449 plot(case_1_applied_force, fit_R2_1,"LineWidth", 1.2, "Color", [0 0.4470 0.7410])
450 grid on; grid minor
451 plot(P1,P1/4)
452 plot(222.4,55.63,'ok')
453 xlabel('Applied Force [N]')
454 ylabel('F1 Reaction Force [N]')
455 hold off
456 subplot(3,1,3)
457 title('Reactions Forces at F2')
458 hold on
459 plot(case_1_applied_force, fit_R3_1,"LineWidth", 1.2, "Color", [0 0.4470 0.7410])
460 grid on; grid minor
461 plot(P1,P1/2)
462 plot(222.4,111.19,'ok')
463 xlabel('Applied Force [N]')
464 ylabel('F2 Reaction Force [N]')
465 Lgnd = legend('Experimental', 'Analytical', 'ANSYS', 'Location', 'bestoutside');

```

```

466 Lgnd.Position(1) = 0.75;
467 Lgnd.Position(2) = 0.45;
468 hold off
469 print('rf comparison','-r300','-dpng')
470
471 % Internal Forces
472
473 figure(7)
474 hold on
475 grid on; grid minor
476 plot(case_1_applied_force, fit_I_1,"LineWidth", 1.2, "Color", [0 0.4470 0.7410])
477 plot(P1,P1)
478 plot(222.4,450.14,'ok')
479 xlabel('Applied Load [N]')
480 ylabel('Displacement [mm]')
481 title('Comparison of Internal Forces For All 3 Models ')
482 legend('Experimental','Analytical','ANSYS','Location','northwest')
483 hold off
484 print('internal comparison','-r300','-dpng')
485
486 % Displacement
487
488 figure(8)
489 hold on
490 plot(case_1_applied_force, fit_D_1,"LineWidth", 1.2, "Color", [0 0.4470 0.7410])
491
492 v_x_case1 = abs((1/(E*I) * (P1/12 * x.^3 - P1.*x)) .* 1000);
493 grid on; grid minor
494 plot(P1,v_x_case1)
495 plot(222.4,1.85,'ok')
496 xlabel('Applied Load [N]')
497 ylabel('Displacement [mm]')
498 title('Comparison of Displacement For All 3 Models ')
499 legend('Experimental','Analytical','ANSYS','Location','northwest')
500 hold off
501 print('displacement comparison','-r300','-dpng')
502
503 %% Plots Question 3
504
505 % First Case
506 figure(9)
507 subplot(2,1,1)
508 plot(case_2_applied_force(1:60,:), case_2_inline_load_cells(1:60,:), "LineWidth", 1.2)
509 title("Internal Force vs Applied Load")
510 xlabel("Applied Load [N]")
511 ylabel("Internal Force [N]")
512 grid on; grid minor
513 subplot(2,1,2)
514 plot(case_2_applied_force(1:60,:), case_2_LVDT(1:60,:), "LineWidth", 1.2)
515 title("Displacement vs Applied Load")
516 xlabel("Applied Load [N]")
517 ylabel("Displacement [mm]")
518 grid on; grid minor
519 print('case 2','-r300','-dpng')
520 % Second Case
521 figure(10)
522 subplot(2,1,1)
523 plot(case_3_applied_force(1:40,:), case_3_inline_load_cells(1:40,:), "LineWidth", 1.2)
524 title("Internal Force vs Applied Load")

```



```

525 xlabel("Applied Load [N]")
526 grid on; grid minor
527 ylabel("Internal Force [N]")
528 subplot(2,1,2)
529 plot(case_3_applied_force(1:40,:), case_3_LVDT(1:40,:), "LineWidth", 1.2)
530 title("Displacement vs Applied Load")
531 xlabel("Applied Load [N]")
532 ylabel("Displacement [mm]")
533 grid on; grid minor
534 print('case 3', '-r300', '-dpng')

```